Numerical solution of the problem of the computational time reversal in the quadrant

Michael V. Klibanov[1], Sergey I. Kabanikhin[2], Dmitrii V. Nechaev[3]

September 21, 2005

The problem of the computational time reversal is posed as the inverse problem of the determination of an unknown initial condition with a finite support in a hyperboilc equation, given the Cauchy data at the lateral surface. A stability estimate for this ill-posed problem implies refocusing of the time reversed wave field. Two such two-dimensional inverse problems are solved numerically in the case when the domain is a quadrant and the Cauchy data are given at finite parts of coordinate axis. The previously obtained Lipschitz stability estimate (if proven) rigorously explains and numerical results confirm the experimentally observed phenomenon of refocusing of time reversed wave fields.

1 Introduction

1.1 Statement of the inverse problem

This is the first publication in which the problem of computational time reversal is solved numerically via the solution of an inverse problem for a hyperbolic equation with the Cauchy data at a lateral surface. Consider the standard Cauchy problem for the hyperbolic equation

$$u_{tt} = Lu \qquad (\boldsymbol{r}, t) \in \mathbb{R}^n \times (0, T), \tag{1.1}$$

$$u\big|_{t=0} = \varphi, \qquad u_t\big|_{t=0} = \psi, \tag{1.2}$$

where L is the elliptic operator of the second order in $\mathbb{R}^n$ with coefficients independent on t, the function $\varphi \in H^2(\mathbb{R}^n)$ and the function $\psi \in H^1(\mathbb{R}^n)$. Hence, the Cauchy problem (1), (2) has unique solution $u \in H^2(\mathbb{R}^n \times (0, T))$. The initial conditions φ and ψ are assumed to have a finite support $D \subset \mathbb{R}^n$,

$$\sup \varphi \subset D, \qquad \sup \psi \subset D. \tag{1.3}$$

We are interested in the following

Inverse Problem 1. Let $\Gamma \subset \mathbb{R}^n$ be a hypersurface and $\Gamma_T = \Gamma \times (0, T)$. Assume that one of initial conditions φ or ψ is known and another one is unknown. Determine that unknown initial condition assuming that the following functions h and g are given

$$u\big|_{\Gamma_T} = h, \qquad \frac{\partial u}{\partial n}\Big|_{\Gamma_T} = g. \tag{1.4}$$

Below we call the problem of recovering of the function φ "the φ-problem", and the problem of recovering of the function ψ "the ψ-problem". Since (1.4) is the Cauchy data, then the Inverse Problem 1 is a particular case of the so-called *Cauchy problem for the hyperbolic equation with the lateral data.* Uniqueness and stability results for this problem are obtained via Carleman estimates and can be found in, e.g., books of Klibanov and Timonov [9] and Lavrentiev, Romanov and Shishatskii [12], as well as in papers of Klibanov and Malinsky [7], Kazemi and Klibanov [5] and Klibanov [6]. The Hölder stability estimate was established in [12] and the stronger Lipschitz stability estimate for bounded domains was proven in [9, 7, 5]. Klibanov [6] has studied both φ- and ψ-problems for a general hyperbolic equation (1.1) with variable coefficients (including hyperbolic inequalities) for $n = 2, 3$, assuming that the domain D is either a quadrant in the 2-D case or an octant in the 3-D case. In the case of the quadrant the data (1.4) were given on finite parts of coordinate

[1]Department of Mathematics and Statistics, University of North Carolina at Charlotte, Charlotte, NC 28223, U.S.A. E-mail: mklibanv@email.uncc.edu

[2]Sobolev Institute of Mathematics, Prospect Acad. Koptyuga 2, Novosibirsk, 630090, Russia. E-mail kabanikh@math.nsc.ru

[3]Lavrent'ev Institute of Hydrodynamics, Prospect Acad. Lavrent'eva 15, Novosibirsk, 630090, Russia. E-mail: nechaev@hydro.nsc.ru

axis, and they were given on finite parts of coordinate planes in the case of the octant. Using previous results of [9, 7, 5], he has proven the Lipschitz stability estimate for this problem, has shown its connection with the refocusing of time reversed wave fields and has proposed a convergent numerical method. Note that the Lipschitz stability in an unbounded domain such as quadrant or octant is rather surprising, since, unlike the bounded domain case, a large part of the energy never reaches the surface (curve in 2-D) where measurements of the wave field and its normal derivative are taken.

The authors are aware only about two publications in which numerical solutions of similar problems were presented. The first one is of Klibanov and Rakesh [10], in which the method of quasi-reversibility of Lattes and Lions [11] was adapted for the solution of the Cauchy problem (1.1), (1.4) with $L = \Delta = \partial_x^2 + \partial_y^2$ in the square with the lateral Cauchy data at the boundary of this square (it was shown in the recent book [9] that the quasi-reversibility is a particular case of the Tikhonov regularization method, and convergence rates were established, also, see [6]). A quite good robustness of this method was demonstrated computationally in [10]. This, observation goes along well with computational results of the current publication and might likely be atributed to the existence of *a priori* Lipschitz stability estimate, which is the best possible one, also see Section 6. The second publication is of Kabanikhin, Bektemesov and Nechaev [4]. They have considered the inverse φ-problem in the 2-D case assuming that $L = \Delta = \partial_x^2 + \partial_y^2$,

$$D = \{(x, y) \mid x \in (0, a), y \in (-b, b)\},$$

$T = a$ and Γ is a part of the $y-$axis,

$$\Gamma = \{(x, y) \mid x = 0, y \in (-b - T, b + T)\}.$$

A uniqueness result for this problem was established and numerical simulations were conducted in this reference.

The present paper is motivated by [6]. We consider the numerical solution of the problem of [6] in the quadrant. To do this, we specify the Inverse Problem 1 as follows.

Inverse Problem 2. Let the function $u(x, y, t)$ be the solution of the standard Cauchy problem (1.1), (1.2) in $\mathbb{R}^2 \times (0, T)$ with $L = \Delta = \partial_x^2 + \partial_y^2$. Suppose that in (1.3) the domain D is the rectangle located in the first quadrant,

$$D = \{(x, y) \mid x \in (0, a), y \in (0, b)\}.$$

Let $\Gamma = \Gamma_1 \cup \Gamma_2$, where Γ_1 and Γ_2 are parts of coordinate axis (see Figure 1):

$$\Gamma_1 = \{x = 0,\ y \in (0, b + T)\}, \qquad \Gamma_2 = \{y = 0,\ x \in (0, a + T)\}.$$

Given functions h and g in (1.4), determine either the function φ assuming that $\psi \equiv 0$ or the function ψ assuming that $\varphi \equiv 0$.

Using (1.3) and the finite speed of propagation of the wave field, we arrive at

$$u\big|_{\partial\Omega} = 0, \qquad t \in (0, T), \tag{1.5}$$

where the domain Ω is

$$\Omega = \{(x, y) \mid x \in (-a - T, a + T), y \in (-b - T, b + T)\}.$$

For $i = 1, 2$ let

$$\Gamma_{iT} = \Gamma_i \times (0, T), \qquad h_i = h\big|_{\Gamma_{iT}}, \quad g_i = g\big|_{\Gamma_{iT}}.$$

We specify conditions (1.4) as follows

$$u\big|_{\Gamma_{1T}} = h_1, \qquad u_x\big|_{\Gamma_{1T}} = g_1, \tag{1.6}$$

$$u\big|_{\Gamma_{2T}} = h_2, \qquad u_y\big|_{\Gamma_{2T}} = g_2, \tag{1.7}$$

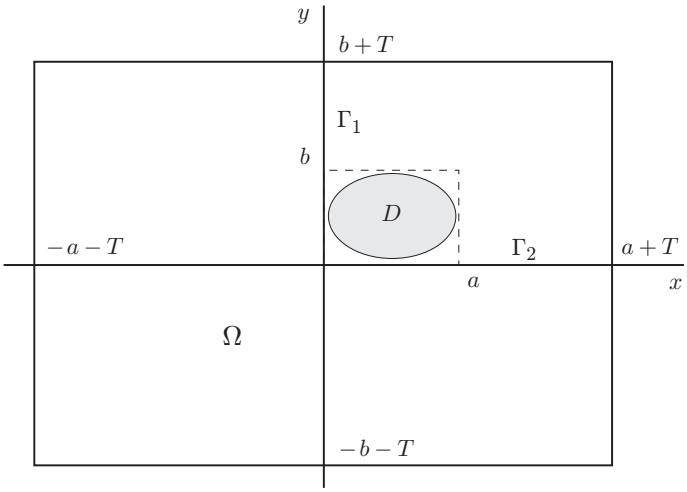

Figure 1: The geometry of the problem

1.2 Connection with time reversal

Borcea, Papanicolaou, Tsogka and Berriman [2] were the first ones who draw the attention of the mathematical community to the issue of the computational time reversal (the mathematical model of [2] is quite different from ours). Bardos and Fink [1] were the first ones who have noticed the direct connection between the problem of the computational time reversal and the Inverse Problem 1. Later this was also observed by Klibanov and Timonov in [9, 8]. The direct linkage between stability results for the Inverse Problem 1 and refocusing in time reversal was first observed in [6].

The set up for the time reversal experiment is well described in the review paper of Fink and Prada [3]. A point source at the moment of time $t = 0$ causes a wave pulse. As a result, waves propagate in $\mathbb{R}^3$. At a surface S, both the wave field and its normal derivative are recorded by many transducers for the time period $t \in (0, T)$ (see p. R3 in [3]). Next, the wave field is "send back" from those transducers by the principle "first in-last out". Actually, therefore, "sending back" the wave field means that experimentalists solve *experimentally* the problem of finding the solution of a hyperbolic equation, given the Cauchy data at S, i. e., given the wave field and its normal derivative at S. However, the initial condition at $\{t = 0\}$ is unknown in this case. Furthermore, the determination of this initial condition via refocusing of the time reversed wave field is actually the main "goal" of the time reversal experiment. Consequently, a direct 3-D analog of the Inverse Problem 1 is solved experimentally. In doing so, an experimental device actually "constructs" the function $v(X, \tau) = \tilde{u}(X, T - \tau)$, $\tau \in (0, T)$, $X \in \mathbb{R}^3$ where $\tilde{u}(X, t)$ is an approximation for the function $u(X, t)$. The major practically interesting phenomenon observed in these experiments is that the time reversed wave field refocuses at the location of the original source. In other words, it replicates the $\delta-$like function, which represents the source of the original pulse.

It is an interesting mathematical problem to explain the refocusing phenomenon *rigorously* and to confirm it numerically. The phenomenon of refocusing in the quadrant is demonstrated numerically in this paper. In terms of the function $v(X, \tau)$, refocusing means that this function at $\tau \approx T$ is close to the δ-function, which represents the original point source. Therefore, to rigorously prove refocusing, one should establish a stability estimate for the Inverse Problem 1. Indeed, a stability estimate guarantees that the approximate solution $\tilde{u}(X, T - \tau)$ should be close to the exact one $u(X, T - \tau)$, as long as the measurement error in the data at the surface S is sufficiently small. Hence, the function $v(X, \tau) = \tilde{u}(X, T - \tau) \approx u(X, T - \tau)$ should be close to the original δ-function at $\tau \approx T$. Consequently, the Lipschitz stability estimate of the paper [6] in the quadrant ensures both a high degree of refocusing in the quadrant and a good stability property of the numerical solution of the Inverse Problem 2. We observe the latter in numerical experiments (Sections 5 and 6). We also mention that previous Lipschitz stability estimates of [9, 7, 5] were obtained for the case when the lateral Cauchy data are given at the boundary of a bounded domain and solution is sought for inside this domain. Thus, they imply a high degree of refocusing of time reversed wave fields propagating in bounded domains.

1.3 The Cauchy problem with the lateral data is not equivalent with the Inverse Problem 1

Although the Inverse Problem 1 is a particular case of the above mentioned Cauchy problem (1.1), (1.4) for the hyperbolic equation with the Cauchy data at a lateral surface, but these problems are not equivalent. Indeed, consider, for example the 1-D case. Let the function $w(x,t)$ be the solution of the standard Cauchy problem

$$w_{tt} = w_{xx}, \qquad (x,t) \in \mathbb{R} \times (0,T),$$

$$w(x,0) = \alpha(x), \qquad w_t(x,0) = \beta(x),$$

where $\alpha \in H^2(\mathbb{R})$ and $\beta \in H^1(\mathbb{R})$. Suppose that the following two functions $f_1(t)$ and $f_2(t)$ represent the lateral Cauchy data at $\{x = 0\}$

$$w(0,t) = f_1(t), \qquad w_x(0,t) = f_2(t), \qquad t \in (0,T).$$

By the D'Alembert formula,

$$w(x,t) = \frac{\alpha(x-t) + \alpha(x+t)}{2} + \frac{1}{2} \int\limits_{x-t}^{x+t} \beta(\xi)\, d\xi.$$

Let $\alpha(x) = \beta(x) = 0$ for $x < 0$. Then we obtain

$$f_1(t) = \frac{\alpha(t)}{2} + \frac{1}{2} \int\limits_0^t \beta(\xi) d\xi, f_2(t) = \frac{\alpha'(t) + \beta(t)}{2}.$$

These two equations are not independent ones, since the second equation can be obtained from the first via the differentiation. Therefore, because of the presence of two unknown functions α and β, the latter system has infinitely many solutions if $f_1'(t) = f_2(t)$ and has no solutions if $f_1'(t) \neq f_2(t)$.

The fact that functions $f_1(t)$ and $f_2(t)$ are actually not independent from each other has the following explanation. Suppose that the hypersurface Γ in the Inverse Problem 1 is the boundary of a certain domain $G \subset \mathbb{R}^n$ and $D \subset G$ (G can be both bounded or unbounded, in the case of the above example $G = \{x > 0\}$). One can uniquely solve the boundary value problem for the equation (1.1) with the zero initial condition at $\{t = 0\}$ and with the Dirichlet boundary condition $u|_{\Gamma_T} = h$ in the domain $(\mathbb{R}^n \setminus G) \times (0,T)$. Solution of this problem uniquely determines the function g in (1.4).

Another explanation of this example of the non-uniqueness is that being given for $t \in (0,T)$, functions $f_1(t)$ and $f_1(t)$ determine the function $w(x,t)$ uniquely only in characteristic triangles $\{x > 0,\, x < t < T - x\}$ and $\{x < 0,\, -x < t < x + T\}$ in the (x,t)-plane, and the axis $\{t = 0\}$ intersects with these triangles only at the origin. On the other hand, assume, for example that the function $\alpha(x) \equiv 0$. Then the function $w(x,t)$ has the odd extension $\tilde{w} \in H^2(\mathbb{R} \times (0,T))$ in $\{t < 0\}$, so as functions $f_1(t)$ and $f_2(t)$. In both cases characteristic triangles become $\{x > 0,\, x - T < t < -x + T\}$ and $\{x < 0,\, -x - T < t < x + T\}$. Since the interval $\{t = 0,\, 0 < x < T\}$ is the median of the first triangle and the interval $\{t = 0 - T < x < 0\}$ is the median of the second, then the function $\beta(x)$ can be determined uniquely in this case. In the case $\beta(x) \equiv 0$ we obtain the even extension and repeat these arguments.

Thus, the uniqueness of the Cauchy problem with the lateral data does not necessarily imply uniqueness of the inverse problem of the determination of initial conditions. This means that the title of this subsection is true. This discussion also demonstrates that it is unlikely that both initial conditions φ and ψ can be determined simultaneously in Inverse Problem 1 and 2, at least in the case when Γ is the boundary of an unbounded domain. This justifies statements of Inverse Problems 1 and 2. Note, however that this issue is a subtle one. Indeed, if, for example Γ is the boundary of a bounded domain and both initial conditions φ and ψ are sought for in this domain, then results of [9, 7, 5] imply that both these initial conditions can be determined uniquely and simultaneously.

2 Numerical method for the direct problem

To solve the direct problem (1.1), (1.2), (1.5), we use the method proposed in [4]. The zero boundary conditions (1.5) allows us to represent the solution in the form of the Fourier sinus-series

$$u(x,y,t) = \sum_{nm} u_{nm}(t) X_n(x) Y_m(y), \tag{2.1}$$

$$X_n(x) = \sin \frac{\pi n(x+a+T)}{2(a+T)}, \qquad Y_m(y) = \sin \frac{\pi m(y+b+T)}{2(b+T)}. \tag{2.2}$$

Substituting (2.1) in (1.1), (1.2), for $u_{nm}(t)$ we obtain the following problem

$$u''_{nm} = \omega^2_{nm} u_{nm}, \qquad \omega^2_{nm} = \frac{\pi^2 n^2}{4(a+T)^2} + \frac{\pi^2 m^2}{4(b+T)^2}, \tag{2.3}$$

$$u_{nm}(0) = \varphi_{nm}, \qquad u'_{nm}(0) = \psi_{nm}, \tag{2.4}$$

where φ_{nm}, ψ_{nm} are respectively the Fourier coefficients of the functions $\varphi(x,y)$ and $\psi(x,y)$,

$$\varphi_{nm} = \frac{1}{(a+T)(b+T)} \int_\Omega \varphi(x,y) X_n(x) Y_m(y)\, dx\, dy, \tag{2.5}$$

$$\psi_{nm} = \frac{1}{(a+T)(b+T)} \int_\Omega \psi(x,y) X_n(x) Y_m(y)\, dx\, dy. \tag{2.6}$$

The solution to the problem (2.3), (2.4) is

$$u_{nm}(t) = \varphi_{nm} \cos(\omega_{nm} t) + \frac{\psi_{nm}}{\omega_{nm}} \sin(\omega_{nm} t). \tag{2.7}$$

Taking into account (2.1), we obtain the following formula for solution to the direct problem

$$u(x,y,t) = \sum_{nm} \Big(\varphi_{nm} \cos(\omega_{nm} t) + \frac{\psi_{nm}}{\omega_{nm}} \sin(\omega_{nm} t) \Big) X_n(x) Y_m(y). \tag{2.8}$$

This formula can be written in the operator's form

$$u = A\boldsymbol{q}, \tag{2.9}$$

where A is a linear operator, $\boldsymbol{q}$ is the vector of Fourier coefficients of the function φ in the φ-problem and of the function ψ in the ψ-problem.

3 Numerical method for the inverse problem

Let $f = (h, g)$ be the vector function representing the data (1.4) for the inverse problem. The Inverse Problem 2 is a linear inverse problem. Hence, it is natural to solve it via the minimization of an objective functional $J[q, f]$ with respect to q. In our case the functional $J[q, f]$ consists of two functionals,

$$J = J_f + J_s, \tag{3.1}$$

where J_f estimates the fulfillment of the conditions (1.6) and (1.7) and J_s estimates fulfillment of condition $\sup q \in D$.

The functional J_f consists of four functionals

$$J_f = J_{h_1} + J_{g_1} + J_{h_2} + J_{g_2}, \tag{3.2}$$

where functionals J_{h_1}, J_{g_1}, J_{h_2}, J_{g_2} respectively estimate fulfillments of conditions $u|_{\Gamma_{1T}} = h_1$, $u_x|_{\Gamma_{1T}} = g_1$, $u|_{\Gamma_{2T}} = h_2$, $u_y|_{\Gamma_{2T}} = g_2$.

The functional J_s has the form

$$J_s[q] = (\|q\|_\Omega^2 - \|q\|_D^2)/2 = (\boldsymbol{q}, S_s\boldsymbol{q})/2, \tag{3.3}$$

where S_s is a symmetric non-negative matrix with elements

$$S_{s,nmlk} = (a+T)(b+T)\delta_{nl}\delta_{mk} - X^a_{nl}Y^b_{mk}. \tag{3.4}$$

Introduce operators A_{h_1}, A_{g_1}, A_{h_2}, A_{g_2} such that

$$\begin{aligned} A_{h_1}\boldsymbol{q} &= (A\boldsymbol{q})\big|_{\Gamma_{1T}}, \qquad & A_{g_1}\boldsymbol{q} &= (A\boldsymbol{q})_x\big|_{\Gamma_{1T}}, \\ A_{h_2}\boldsymbol{q} &= (A\boldsymbol{q})\big|_{\Gamma_{2T}}, \qquad & A_{g_2}\boldsymbol{q} &= (A\boldsymbol{q})_y\big|_{\Gamma_{2T}}. \end{aligned} \tag{3.5}$$

Let $\|\cdot\|$ denotes the L_2-norm. We can write the expression for J_{h_1} as follows

$$J_{h_1}[q,f] = \|A_{h_1}\boldsymbol{q} - h_1\|^2/2 = \|A_{h_1}\boldsymbol{q}\|^2/2 - \langle A_{h_1}\boldsymbol{q}, h_1\rangle + \|h_1\|^2/2 = (\boldsymbol{q}, S_{h_1}\boldsymbol{q})/2 - (\boldsymbol{q}, \boldsymbol{h}_1) + \|h_1\|^2/2, \tag{3.6}$$

where $S_{h_1} = A^*_{h_1}A_{h_1}$ is the symmetric non-negative matrix; $\boldsymbol{h}_1 = A^*_{h_1}h_1$ is the vector, and $(\boldsymbol{v}, \boldsymbol{w})$ denotes the scalar product,

$$(\boldsymbol{v}, \boldsymbol{w}) = \sum_{nm} v_{nm}w_{nm}.$$

The expressions for elements of the matrix S_{h_1} and the vector $\boldsymbol{h}_1$ depend on the problem we consider, i.e., the φ-problem or the ψ-problem. We mark the elements for the φ-problem by the superscript φ and the elements for the ψ-problem by the superscript ψ. Then

$$S^{\varphi}_{h_1,nmlk} = s_n s_l Y^{b+T}_{mk}\Phi^{cc}_{nmlk}, \tag{3.7}$$

$$S^{\psi}_{h_1,nmlk} = s_n s_l Y^{b+T}_{mk}\frac{\Phi^{ss}_{nmlk}}{\omega_{nm}\omega_{lk}}, \tag{3.8}$$

$$h^{\varphi}_{1,nm} = s_n\int_0^{b+T} Y_m(y)\int_0^T \cos(\omega_{nm}t)h_1(y,t)\,dt\,dy, \tag{3.9}$$

$$h^{\psi}_{1,nm} = \frac{s_n}{\omega_{nm}}\int_0^{b+T} Y_m(y)\int_0^T \sin(\omega_{nm}t)h_1(y,t)\,dt\,dy, \tag{3.10}$$

where

$$s_n = X_n(0) = \sin(\pi n/2); \tag{3.11}$$

$$Y^z_{mk} = \int_0^z Y_m(y)Y_k(y)\,dy; \tag{3.12}$$

$$\Phi^{cc}_{nmlk} = \int_0^T \cos(\omega_{nm}t)\cos(\omega_{lk}t)\,dt; \tag{3.13}$$

$$\Phi^{ss}_{nmlk} = \int_0^T \sin(\omega_{nm}t)\sin(\omega_{lk}t)\,dt. \tag{3.14}$$

We obtain analogous expressions for other functionals. We get for J_{g_1}

$$J_{g_1}[q,f] = \|A_{g_1}\boldsymbol{q} - g_1\|/2 = (\boldsymbol{q}, S_{g_1}\boldsymbol{q})/2 - (\boldsymbol{q}, \boldsymbol{g}_1) + \|g_1\|^2/2, \tag{3.15}$$

where $S_{g_1} = A^*_{g_1}A_{g_1}$ is the matrix with elements

$$S^{\varphi}_{g_1,nmlk} = c_n c_l Y^{b+T}_{mk}\Phi^{cc}_{nmlk}\frac{\pi^2 nl}{4(a+T)^2}, \tag{3.16}$$

$$S^{\psi}_{g_1,nmlk} = c_n c_l Y^{b+T}_{mk}\frac{\Phi^{ss}_{nmlk}}{\omega_{nm}\omega_{lk}}\frac{\pi^2 nl}{4(a+T)^2}, \tag{3.17}$$

$$c_n = X_n'(0) = \cos(\pi n/2); \tag{3.18}$$

$\boldsymbol{g}_1 = A_{g_1}^* g_1$ is the vector with components

$$g_{1,nm}^{\varphi} = \frac{\pi c_n n}{2(a+T)} \int_0^{b+T} Y_m(y) \int_0^T \cos(\omega_{nm} t) g_1(y,t)\, dt\, dy, \tag{3.19}$$

$$g_{1,nm}^{\psi} = \frac{\pi c_n n}{2(a+T)\omega_{nm}} \int_0^{b+T} Y_m(y) \int_0^T \sin(\omega_{nm} t) g_1(y,t)\, dt\, dy. \tag{3.20}$$

We obtain for J_{h_2}

$$J_{h_2}[q] = \|A_{h_2}\boldsymbol{q} - h_2\|^2/2 = (\boldsymbol{q}, S_{h_2}\boldsymbol{q})/2 - (\boldsymbol{q}, \boldsymbol{h}_2) + \|h_2\|^2/2, \tag{3.21}$$

where entries of the matrix $S_h = A_{h_2}^* A_{h_2}$ are

$$S_{h_2,nmlk}^{\varphi} = s_m s_k X_{nl}^{a+T} \Phi_{nmlk}^{cc}, \tag{3.22}$$

$$S_{h_2,nmlk}^{\psi} = s_m s_k X_{nl}^{a+T} \frac{\Phi_{nmlk}^{ss}}{\omega_{nm}\omega_{lk}}, \tag{3.23}$$

$$X_{nl} = \int_0^{a+T} X_n(x) X_l(x)\, dx; \tag{3.24}$$

$\boldsymbol{h}_2 = A_{h_2}^* h_2$ is the vector with components

$$h_{2,nm}^{\varphi} = s_m \int_0^{a+T} X_n(x) \int_0^T \cos(\omega_{nm} t) h_2(x,t)\, dt\, dx, \tag{3.25}$$

$$h_{2,nm}^{\psi} = s_m \int_0^{a+T} X_n(x) \int_0^T \sin(\omega_{nm} t) h_2(y,t)\, dt\, dy. \tag{3.26}$$

We obtain for J_{g_2}

$$J_{g_2}[q,f] = \|A_{g_2}\boldsymbol{q} - g_2\|^2/2 = (\boldsymbol{q}, S_{g_2}\boldsymbol{q})/2 - (\boldsymbol{q}, \boldsymbol{g}_2) + \|g_2\|^2/2, \tag{3.27}$$

where $S_{g_2} = A_{g_2}^* A_{g_2}$ is the matrix with entries

$$S_{g_2,nmlk}^{\varphi} = c_m c_k X_{nl}^{a+T} \Phi_{nmlk}^{cc} \frac{\pi^2 mk}{4(b+T)^2}, \tag{3.28}$$

$$S_{g_2,nmlk}^{\psi} = c_m c_k X_{nl}^{a+T} \frac{\Phi_{nmlk}^{ss}}{\omega_{nm}\omega_{lk}} \frac{\pi^2 mk}{4(b+T)^2}; \tag{3.29}$$

$\boldsymbol{g}_2 = A_{g_2}^* g_2$ is the vector with components

$$g_{2,nm}^{\varphi} = \frac{\pi c_m m}{2(b+T)} \int_0^{a+T} X_n(x) \int_0^T \cos(\omega_{nm} t) g_2(y,t)\, dt\, dy, \tag{3.30}$$

$$g_{2,nm}^{\psi} = \frac{\pi c_m m}{2(b+T)\omega_{nm}} \int_0^{a+T} X_n(x) \int_0^T \sin(\omega_{nm} t) g_2(y,t)\, dt\, dy. \tag{3.31}$$

Using (3.6), (3.15), (3.21), (3.27), we obtain the following expression for J_f:

$$J_f = \|A_\Gamma \boldsymbol{q} - f\|^2/2 = (\boldsymbol{q}, S_f \boldsymbol{q})/2 - (\boldsymbol{q}, \boldsymbol{f}) + \|f\|^2/2, \tag{3.32}$$

where A_Γ is the linear operator: $A_\Gamma \boldsymbol{q} = \{A_{h_1}\boldsymbol{q}, A_{g_1}\boldsymbol{q}, A_{h_2}\boldsymbol{q}, A_{g_2}\boldsymbol{q}\}$, $f = \{h_1, g_1, h_2, g_2\}$ is a vector function. $S_f = A_\Gamma^* A_\Gamma$ is a symmetric non-negative matrix

$$S_f = S_{h_1} + S_{g_1} + S_{h_2} + S_{g_2}; \tag{3.33}$$

and $\boldsymbol{f} = A_\Gamma^* f$ denotes the vector

$$\boldsymbol{f} = \boldsymbol{h}_1 + \boldsymbol{g}_1 + \boldsymbol{h}_2 + \boldsymbol{g}_2. \tag{3.34}$$

Combining (3.32) and (3.3), we obtain

$$J[q, f] = J_f[q] + J_s[q] = (\boldsymbol{q}, S\boldsymbol{q})/2 - (\boldsymbol{q}, \boldsymbol{f}) + \|f\|/2, \tag{3.35}$$

where S is a symmetric non-negative matrix with elements

$$S = S_f + S_s. \tag{3.36}$$

It follows from (3.35) that J is a quadratic functional. It is well known that one of the most effective methods of minimization of quadratic functionals is the conjugate gradient method. Thus, we will use it. This method can be schematically described as follows.

1. On the k-th iteration we compute the gradient of J with respect to $\boldsymbol{q}$

$$\boldsymbol{g}_k = \nabla_q J_k = S\boldsymbol{q}_k - \boldsymbol{f}. \tag{3.37}$$

   Suppose that $|\boldsymbol{g}_k| < \varepsilon$, where ε is an *a priori* chosen small number. Then we stop the iterative process and consider the vector $\boldsymbol{q}_k$ as the solution. Otherwise, we go to the next step.

2. Compute the conjugate gradient

$$\boldsymbol{p}_k = \boldsymbol{g}_k - \beta_k \boldsymbol{p}_{k-1}, \qquad \beta_k = (S\boldsymbol{p}_{k-1}, \boldsymbol{g}_k)/(S\boldsymbol{p}_{k-1}, \boldsymbol{p}_{k-1}). \tag{3.38}$$

   For $k = 0$ set $\boldsymbol{p}_0 = \boldsymbol{g}_0$.

3. Calculate the step of descent

$$\alpha_k = (\boldsymbol{p}_k, \boldsymbol{g}_k)/(S\boldsymbol{p}_k, \boldsymbol{p}_k). \tag{3.39}$$

4. Compute the new vector

$$\boldsymbol{q}_{k+1} = \boldsymbol{q}_k - \alpha_k \boldsymbol{p}_k \tag{3.40}$$

   and return to the first step.

It well known that the number of iterations, which is required to reach the minimum of the quadratic functional equals to the dimension of the vector $\boldsymbol{q}$ [14].

To estimate the accuracy of our solution, we refer to the Tikhonov concept of solutions of ill-posed problems, see Tikhonov and Arsenin [13]. By this concept one needs to assume the existence of an "ideal" exact solution with an ideal exact data. Then one should assume that a certain error is perturbing the ideal data, which leads to a non-ideal data, and estimate the difference between the computed solution corresponding that non-ideal data and the exact solution. Thus, we arrive at the following lemma

Lemma 1. *Let $\boldsymbol{q}_*$ be the exact solution of the inverse problem with the exact data $f_* = (h_\star, g_*)$ and $\boldsymbol{q}$ be the minimizer of the functional $J[q, f]$ with the data $f = (h, g)$. Then*

$$\|\boldsymbol{q} - \boldsymbol{q}_*\| \leq \frac{(s_{f,\max})^{1/2} \|f - f_*\| + \|\nabla_q J[q, f]\|}{s_{\min}}, \tag{3.41}$$

$$\|\boldsymbol{q} - \boldsymbol{q}_*\| \leq \frac{\|f - f_*\| + \sqrt{2J[q, f]}}{\sqrt{s_{\min}}}, \tag{3.42}$$

where $s_{f,\max}$ is the maximal eigenvalue of the matrix S_f and $s_{\min}$ is the minimal eigenvalue of the matrix S.

Proof. Since q_* is the exact solution with the exact data we have $J[q_*, f_*] = 0$ and $\nabla_q J[q_*, f_a st] = S\boldsymbol{q}_* - \boldsymbol{f}_* = 0$. Therefore

$$\nabla_q J[q, f] = (S\boldsymbol{q} - \boldsymbol{f}) - (S\boldsymbol{q}_* - \boldsymbol{f}_*) = S(\boldsymbol{q} - \boldsymbol{q}_*) - (\boldsymbol{f} - \boldsymbol{f}_*).$$

Using the triangle inequality, we obtain

$$\|S(\boldsymbol{q} - \boldsymbol{q}_*)\| \le \|\boldsymbol{f} - \boldsymbol{f}_*\| + \|\nabla_q J[q, f]\|.$$

Taking into account the inequalities

$$\|\boldsymbol{f} - \boldsymbol{f}_*\| = \|A_\Gamma^*(f - f_*)\| \le \sqrt{s_{f,\max}}\, \|f - f_*\|,$$

$$\|S(\boldsymbol{q} - \boldsymbol{q}_*)\| \ge s_{\min} \|\boldsymbol{q} - \boldsymbol{q}_*\|,$$

we obtain (3.41).

To prove (3.42), consider the gradient of J with respect to f,

$$\nabla_f J[q, f] = f - A_\Gamma \boldsymbol{q}.$$

Since $f_* = A_\Gamma \boldsymbol{q}_*$, we have

$$\nabla_f J[q, f] = (f - A_\Gamma \boldsymbol{q}) - (f_* - A_\Gamma \boldsymbol{q}_*) = (f - f_*) - A_\Gamma(\boldsymbol{q}_1 - \boldsymbol{q}_2).$$

Using the triangle inequality, we obtain

$$\|A_\Gamma(\boldsymbol{q} - \boldsymbol{q}_*)\| \le \|f - f_*\| + \|\nabla_f J[q, f]\|,$$

which with relations

$$\|A_\Gamma(\boldsymbol{q} - \boldsymbol{q}_*)\| \ge \sqrt{s_{\min}}\, \|\boldsymbol{q} - \boldsymbol{q}_*\|,$$

$$\|\nabla_f J[q]\| = \|f - A_\Gamma \boldsymbol{q}\| = \sqrt{2J[q, f]},$$

yields (3.42).

Remark 1. Note that the gradient of the objective functional with respect to the data is used in the proof of this lemma. The authors are not aware about other publications which would employ this idea.

4 Numerical results

We solve numerically both φ- and ψ-problems for the test function $q_*(x, y)$ given by

$$q_*(x, y) = \begin{cases} \sin(2\pi x/a) \sin(2\pi y/b), & (x, y) \in D; \\ 0, & (x, y) \notin D. \end{cases}$$

The following values of parameters are taken: $a = 1$, $b = 1$, $T = 1.5$, i. e. $D = (0, 1) \times (0, 1)$, $\Omega = (-2.5, 2.5) \times (-2.5, 2.5)$ (see Figure 2). The domain Ω is partitioned in $M = 2^6 = 64$ equal parts with respect to the variable y and in $N = 2^6 = 64$ equal parts with respect to x. The time interval $(0, T)$ is partitioned in $K = 100$ equal parts.

First, we solve the direct problem and compute the functions $\{h_{1*}, g_{1*}, h_{2*}, g_{2*}\} = f_*$. Figure 3 illustrates the functions h_{2*}, g_{2*} ($h_{1*} = h_{2*}$, $g_{1*} = g_{2*}$ due to the symmetry) for φ- and ψ-problems respectively.

Next, we solve the inverse problem with the data $f = f_*$. Each of the integrals entering the expressions for entries of the matrices S_{h_1}, S_{g_1}, S_{h_2}, S_{g_2}, S_s and vectors $\boldsymbol{h}_1$, $\boldsymbol{g}_1$, $\boldsymbol{h}_2$, $\boldsymbol{g}_2$ (see the previous section) is approximated by the sum

$$\int u(x)\, dx \approx \Delta x \sum u(n\, \Delta x),$$

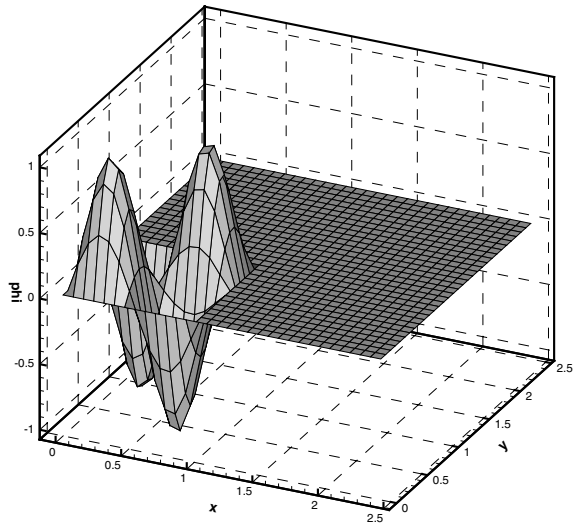

Figure 2: The test function $q_*(x, y)$

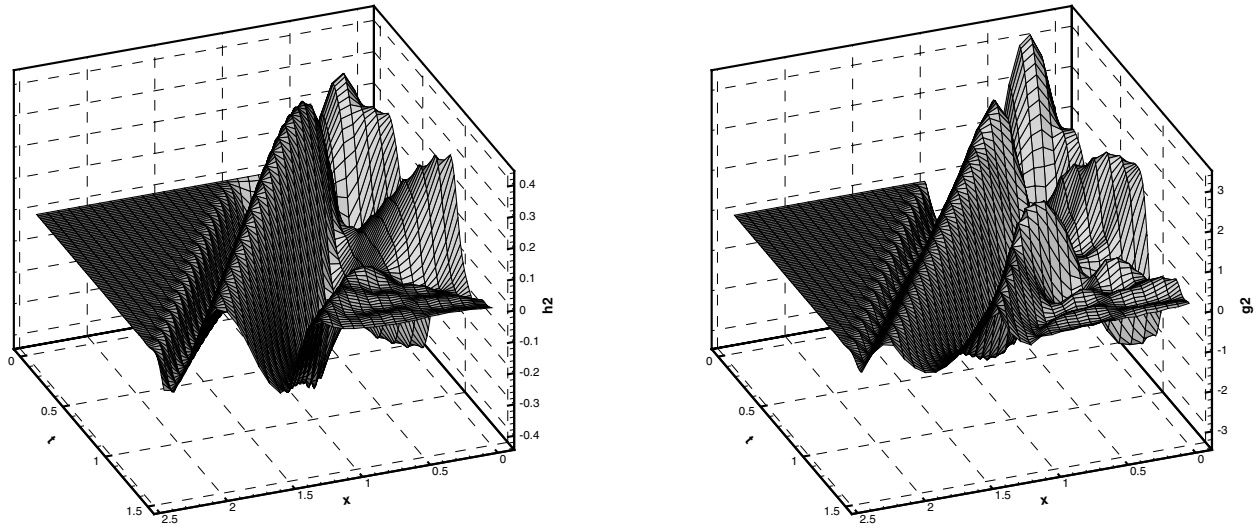

Figure 3: Solution of the direct problem: $h_{2*}(x, t)$ (left); $g_{2*}(x, t)$ (right)

where Δx is the discretization step. Using $q = 0$ as the initial guess, we proceed with the conjugate gradient method as long as either the number of iterations is less than 300 or the norm of the gradient of the functional is exceeds 10^{-10}.

The results of the numerical solution of φ- and ψ-problem are presented on Figures 4, 5 respectively. One can see that in order to solve the ψ-problem, only 30 iterations are required to reach $\|\nabla_q J\| < 10^{-10}$. Whereas the norm of the gradient of the functional for the φ-problem $\|\nabla J_q\| \approx 2 \cdot 10^{-2}$ after 300 iterations. To explain this difference, we consider the eigenvalues of matrices. The results of numerical computations of the eigenvalues are presented in Table 1. It follows that the condition number ($\chi = s_{\max}/s_{\min}$) of the matrix $S_f + S_s$ for the φ-problem is $\chi^\varphi = 8903/6.536 \approx 1362$, while the condition number for the ψ-problem is $\chi^\psi = 9.605/0.832 \approx 11.5$. Therefore, χ^φ almost 100 times greater than χ^ψ, which explains why the convergence rate for the ψ-problem is much better than for the φ-problem.

Remark 2. As it was mentioned above in the description of the algorithm for the inverse problem, to achieve the minimum it is required $\dim \boldsymbol{q}$ iterations. In our case $\dim \boldsymbol{q} = NM = 64 \cdot 64 = 4096$. However, we achieve the minimum after about 100 iterations, which is a very good number. We cannot yet fully explain this.

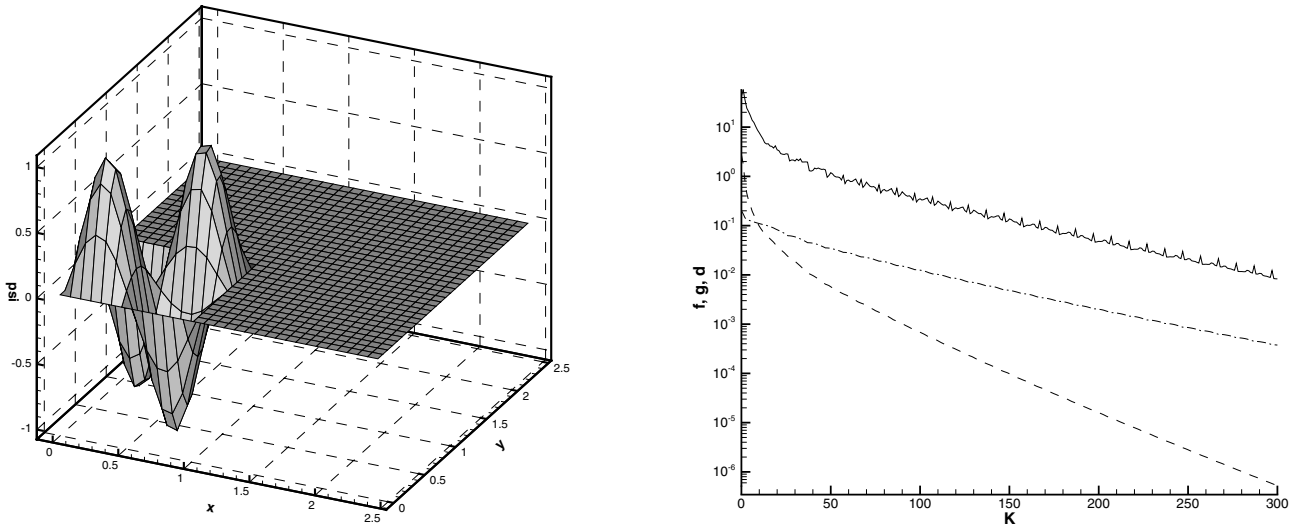

Figure 4: Solution of the φ-problem (left) and dependencies of the norm of the gradient of functional $\|\nabla_q J[\varphi_k, f_*]\|$ (solid curve), the functional $J[\varphi_k, f_*]$ (dashed curve), the norm of deviation from the exact solution $\|\boldsymbol{\varphi}_k - \boldsymbol{\varphi}_*\|$ (dash-dotted curve) on the iteration number k (right)

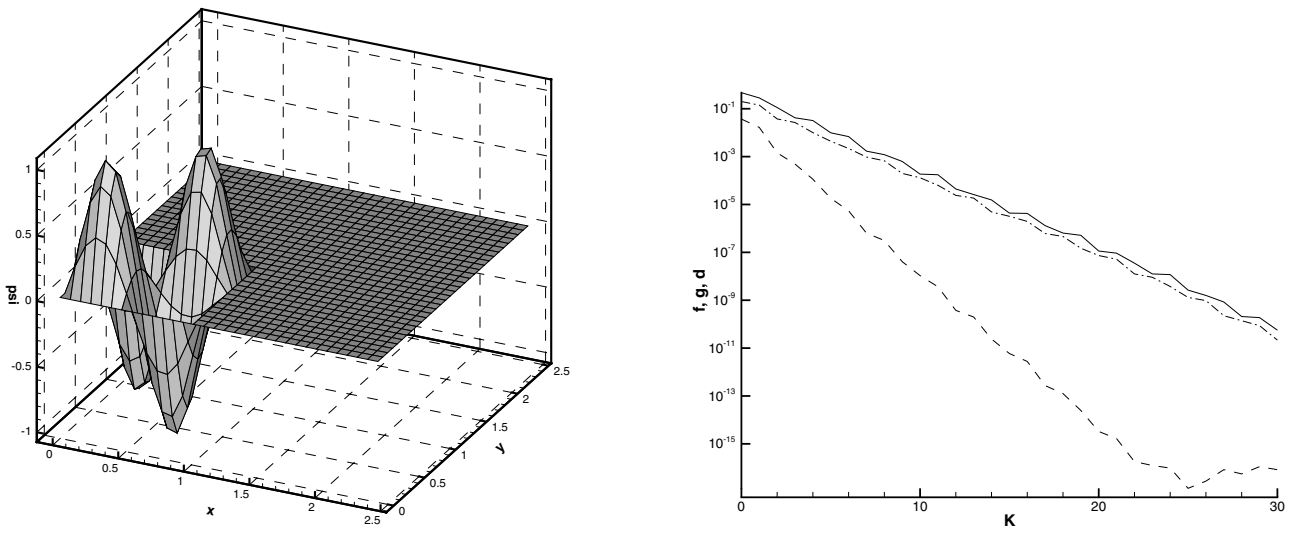

Figure 5: Solution of the ψ-problem (left) and dependencies of the norm of the gradient of functional $\|\nabla_q J[\psi_k, f_*]\|$ (solid curve), the functional $J[\psi_k, f_*]$ (dashed curve), the norm of deviation from the exact solution $\|\boldsymbol{\psi}_k - \boldsymbol{\psi}_*\|$ (dash-dotted curve) on the iteration number k (right)

Table 1: The eigenvalues of matrices

S	$s_{\min}$	$s_{\max}$
S_s	0	6.25
S_f^{φ}	$1.861 \cdot 10^{-4}$	8900
S_f^{ψ}	$7.988 \cdot 10^{-7}$	3.455
$S_f^{\varphi} + S_s$	6.536	8903
$S_f^{\psi} + S_s$	0.832	9.605

Table 2: The eigenvalues and condition number of the matrix $S^{\varphi}(\gamma)$

γ	$s_{\min}$	$s_{\max}$	χ
0	$1.861 \cdot 10^{-4}$	8900	$4.78 \cdot 10^{7}$
1	6.536	8903	1360
5	16.034	8914	556
10	21.104	8928	423
30	27.569	8984	326
50	29.782	9041	304
100	32.032	9191	287
200	33.567	9518	284
300	34.206	9886	289
1000	35.320	13563	384
10000	35.881	69547	1940
100000	35.945	628557	17500

Table 3: The eigenvalues and condition number of the matrix $S^{\psi}(\gamma)$

γ	$s_{\min}$	$s_{\max}$	χ
0	$7.988 \cdot 10^{-7}$	3.455	$4.325 \cdot 10^{7}$
0.1	0.281	4.023	14.27
0.2	0.498	4.638	9.304
0.3	0.628	5.257	8.360
0.4	0.692	5.879	8.496
0.5	0.734	6.501	8.853
0.6	0.764	7.123	9.312
0.7	0.787	7.745	9.828
1	0.832	9.605	11.53
5	0.931	34.24	36.75
10	0.946	65.77	69.52
100	0.959	627.8	654.4

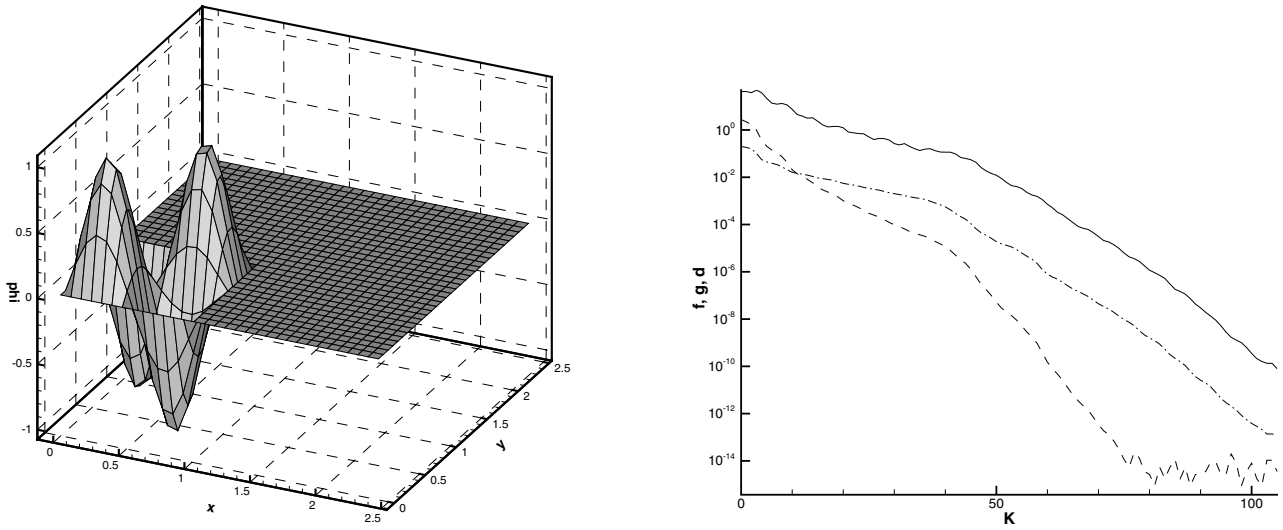

Figure 6: Solution of the φ-problem with $\gamma = 200$ (left) and dependencies of the norm of the gradient of functional $\|\nabla_q J[\psi_k, f_*]\|$ (solid curve), the functional $J[\psi_k, f_*]$ (dashed curve), the norm of deviation from the exact solution $\|\boldsymbol{\psi}_k - \boldsymbol{\psi}_*\|$ (dash-dotted curve) on the iteration number k (right)

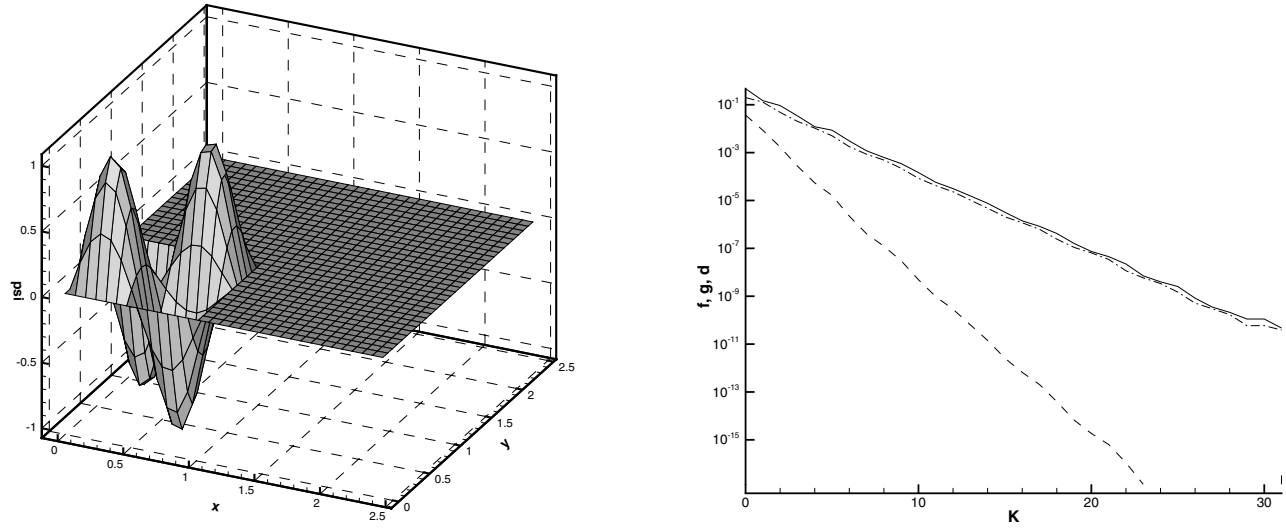

Figure 7: Solution of the ψ-problem with $\gamma = 0.3$ (left) and dependencies of the norm of the gradient of functional $\|\nabla_q J[\psi_k, f_*]\|$ (solid curve), the functional $J[\psi_k, f_*]$ (dashed curve), the norm of deviation from the exact solution $\|\boldsymbol{\psi}_k - \boldsymbol{\psi}_*\|$ (dash-dotted curve) on the iteration number k (right)

To decrease the condition number χ, we consider the following functional

$$J(\gamma) = J_f + \gamma J_s, \tag{4.1}$$

where γ is a parameter. Dependencies of eigenvalues and the condition number of the matrix $S(\gamma) = S_f + \gamma S_s$ on the parameter γ for φ- and ψ-problems are presented in Tables 2 and 3 respectively. One can see that the minimal condition number $\chi^{\varphi}_{\min} = 284$ for the φ-problem is reached when $\gamma^{\varphi}_{\min} = 200$, while for the ψ-problem $\chi^{\psi}_{\min} = 8.36$ is reached when $\gamma^{\psi}_{\min} = 0.3$.

Figure 6 illustrates the numerical solution of the φ-problem with $\gamma = 200$, and Figure 7 illustrates the numerical solution of the ψ-problem with $\gamma = 0.3$. The convergence rate of the φ-problem is notably improved, since only 106 iterations is required now to reach $\|\nabla_q J[q, f]\| < 10^{-10}$. The convergence rate of the ψ-problem did not change, because the condition number for $\gamma = 1$ does not differ significantly from the condition number for $\gamma = 0.3$ (see Table 3).

5 The case of a random noise in the data

To estimate the influence of the random noise in the data f on the solution of the inverse problem, we introduce this noise in the data and solve the resulting inverse problem. So, the precise data f_* is replaced with the noisy data f_ε as

$$f_{\varepsilon,kn} = (1 + \varepsilon \operatorname{rnd}())f_{*,kn},$$

where ε is the noise level and rnd () is the result of the random number generator with the normal distribution in $[-1, 1]$.

Tables 4, 5 illustrate the results of numerical solutions of both φ- and ψ-problems for various levels ε of the noise. Since $\|\varphi_\star\| = \|\psi_\star\| = 1/2$, then the relative differences can be obtained from norms $\|\varphi - \varphi_\star\|$, $\|\psi - \psi_\star\|$ given in these tables via the multiplication by 5. In addition to the norm of the deviation of the computed solution from the exact one $\|\boldsymbol{q} - \boldsymbol{q}_*\|$, we present the norm of the deviation of the noisy data from the exact one $\|f_\varepsilon - f_*\|$, the value of the functional $J[q]$ and estimates (3.41) and (3.42). The norm of the gradient $\|\nabla_q J\| < 10^{-10}$ at the last iteration for all ε and, therefore is not presented. The values of $s_{f,\max}$, $s_{\min}$ entering estimates (3.41), (3.42) are taken from Table 1 and Tables 2, 3 ($\gamma^{\varphi} = 200$, $\gamma^{\psi} = 0.3$). An interesting feature of these results is that even at $\varepsilon = 0.5$, which corresponds to the 50% random noise in the data the relative difference between computed and exact solutions does not exceed 4% for the $\varphi-$problem and 10% for the $\psi-$ problem.

One can see that the estimate (3.42) is more accurate than (3.41). To explain this, consider the case when the number of iterations is not limited. In this case we would obtain such a solution $\boldsymbol{q}$ that $\|\nabla_q J[q, f_\varepsilon]\| = 0$

Table 4: Deviation of numerical solution for φ-problem with $\varphi_* = \sin(2\pi x/a)\sin(2\pi y/b)$

ε	$\|f_\varepsilon - f_*\|$	$J[\varphi]$	$\|\boldsymbol{\varphi} - \boldsymbol{\varphi}_*\|$	Estimate (3.41)	Estimate (3.42)
0	0	$3.55 \cdot 10^{-15}$	$1.24 \cdot 10^{-13}$	$2.38 \cdot 10^{-12}$	$1.45 \cdot 10^{-8}$
0.001	0.001	$8.27 \cdot 10^{-7}$	$1.29 \cdot 10^{-5}$	0.003	$4.55 \cdot 10^{-4}$
0.005	0.006	$2.09 \cdot 10^{-5}$	$6.35 \cdot 10^{-5}$	0.018	0.002
0.01	0.013	$8.39 \cdot 10^{-5}$	$1.88 \cdot 10^{-4}$	0.038	0.004
0.05	0.066	$2.01 \cdot 10^{-3}$	$6.87 \cdot 10^{-4}$	0.187	0.022
0.1	0.134	$8.17 \cdot 10^{-3}$	$1.53 \cdot 10^{-3}$	0.377	0.045
0.5	0.682	0.210	$7.99 \cdot 10^{-3}$	1.918	0.229

Table 5: Deviation of numerical solution for ψ-problem with $\psi_* = \sin(2\pi x/a)\sin(2\pi y/b)$

ε	$\|f_\varepsilon - f_*\|$	$J[\psi]$	$\|\boldsymbol{\psi} - \boldsymbol{\psi}_*\|$	Estimate (3.41)	Estimate (3.42)
0	0	$5.551 \cdot 10^{-17}$	$3.865 \cdot 10^{-11}$	$7.45 \cdot 10^{-11}$	$1.32 \cdot 10^{-8}$
0.001	$1.57 \cdot 10^{-4}$	$1.129 \cdot 10^{-8}$	$3.408 \cdot 10^{-5}$	$4.64 \cdot 10^{-4}$	$3.87 \cdot 10^{-4}$
0.005	$7.56 \cdot 10^{-4}$	$2.595 \cdot 10^{-7}$	$1.672 \cdot 10^{-4}$	$2.23 \cdot 10^{-3}$	$1.86 \cdot 10^{-3}$
0.01	$1.51 \cdot 10^{-3}$	$1.047 \cdot 10^{-6}$	$3.215 \cdot 10^{-4}$	$4.48 \cdot 10^{-3}$	$3.73 \cdot 10^{-3}$
0.05	$7.76 \cdot 10^{-3}$	$2.709 \cdot 10^{-5}$	$1.854 \cdot 10^{-3}$	0.022	0.019
0.1	0.015	$1.111 \cdot 10^{-4}$	$3.136 \cdot 10^{-3}$	0.046	0.038
0.5	0.076	$2.591 \cdot 10^{-3}$	0.019	0.225	0.187

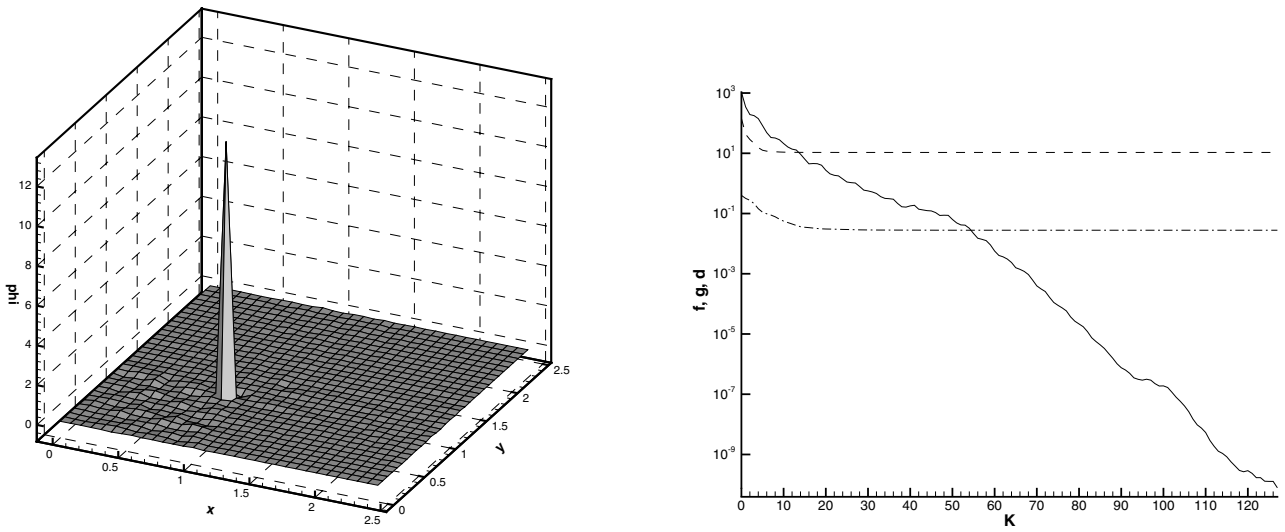

Figure 8: Solution of the φ-problem with $\varepsilon = 0.5$ (left) and dependencies of the norm of the gradient of functional $\|\nabla_q J[\varphi_k, f_\varepsilon]\|$ (solid curve), the functional $J[\varphi_k, f_\varepsilon]$ (dashed curve), the norm of deviation from the exact solution $\|\boldsymbol{\varphi}_k - \boldsymbol{\varphi}_*\|$ (dash-dotted curve) on the iteration number k (right)

and $J[q, f_\varepsilon] \approx \|f_\varepsilon - f\|^2/2$. Then

$$\frac{\|\boldsymbol{q} - \boldsymbol{q}_*\|_{(3.41)}}{\|\boldsymbol{q} - \boldsymbol{q}_*\|_{(3.42)}} \approx \frac{1}{2}\sqrt{\frac{s_{f,\max}}{s_{\min}}}.$$

Therefore, if $s_{f,\max}/s_{\min} > 4$, then the estimate (3.42) is more accurate than (3.41). However, if $s_{f,\max}/s_{\min} < 4$, then the estimate (3.41) is more accurate than (3.42). Since $s_{f,\max}/s_{\min} > 4$ for both φ- and ψ-problems, then the estimate (3.42) should give lesser values than (3.41). It follows from Tables 4, 5 that the computed deviation of the solution is almost 10 times less than one predicted by the estimate (3.42). This may be explained by the smoothness of the exact solution q_*.

We now consider the φ-problem for the δ-like test function $\varphi_*(x, y) = \delta(x-0.9)\delta(y-0.9)$. This is an exact analog of the problem of time reversal. The discrete analog of $\delta(x-0.9)\delta(y-0.9)$ is $\varphi_{*,nm} = \delta_{nn'}\delta_{mm'}/\sqrt{h_x h_y}$, where $\delta_{nn'} = 0$ if $n = n'$ and $\delta_{nn'} = 0$ otherwise; n' is the index of the grid point close to $x = 0.9$; m' is the index of the grid point close to $y = 0.9$; h_x and h_y are discretization steps along the x- and y-axis respectively. Figure 8 illustrates the solution of the problem with the quite high noise level $\varepsilon = 0.5$. The norm of the deviation $\|\boldsymbol{\varphi} - \boldsymbol{\varphi}_*\| = 2.78 \cdot 10^{-2}$, while the estimate (3.42) gives $2.31 \cdot 10^{-1}$. Hence, we have now $\approx 7\%$ of the relative error in the solution at 50% of the random noise in the data. Thus, the high accuracy of numerical solutions cannot be attributed only to the smoothness of the exact solutions. So, we provide some insights of this phenomenon in the next section. We note that Figure 8 demonstrates a quite good refocusing of the time reversed wave field in the presence of a large amount of random noise in the data.

6 Summary

We are motivated by an interesting experimentally observed phenomenon of refocusing of time reversed wave fields [3]. Using a mathematical model of time reversal proposed in [6], we have developed method for the numerical solution of the inverse problem of determining an unknown initial condition in the 2-D wave equation $u_{tt} = u_{xx} + u_{yy}$. The support of the unknown initial condition is in the first quadrant of the $(x, y)-$plane and the lateral Cauchy data are given at finite parts of coordinate axis. A number of numerical results is presented, including the one (Figure 8), which directly models the phenomenon of refocusing in the time reversal experiment. We have estimated convergence rates and accuracy of solutions of our algorithm for both φ- and $\psi-$problems both analytically and numerically. An interesting feature of our computational results is their surprisingly high accuracy even in the presence of a large amount of random noise in the data. Indeed, at 50% noise in the data the relative error of our solutions repeatedly did not exceed a few

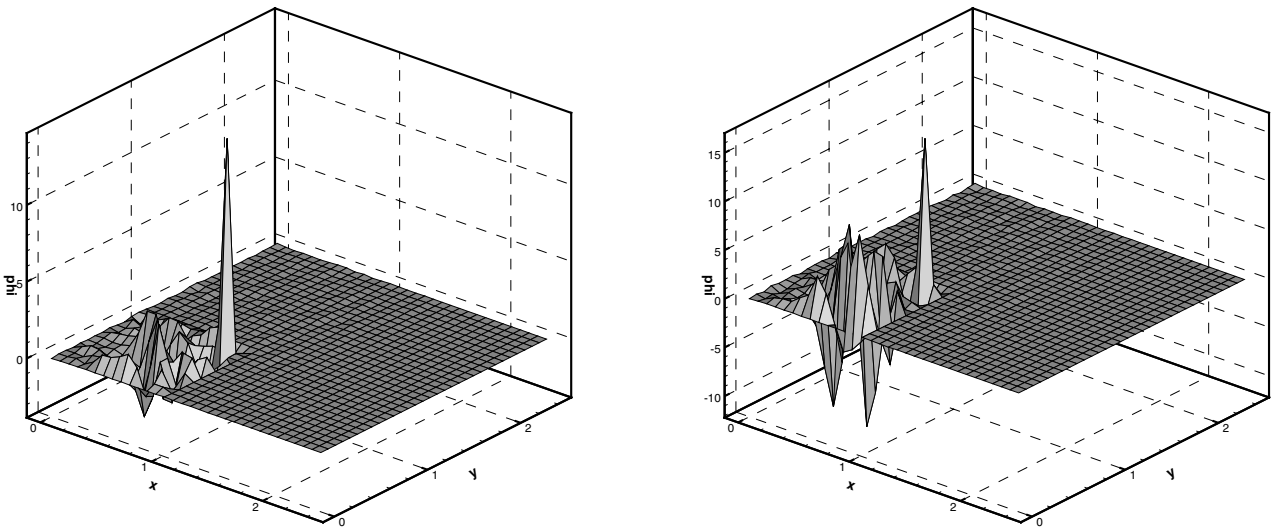

Figure 9: Solution of the φ-problem with $\varepsilon = 0.3$ (left) and $\varepsilon = 0.5$ (right)

per cent. In our opinion, this can be explained by the existence of *a priori* Lipschitz stability estimate [6] for this inverse problem. We recall that the Lipschitz stability estimate is the best possible. Observe that a similar high accuracy in the presence of a large amount of noise in the data was also demonstrated in the much earlier work [10], where the 2-D wave equation was solved with the lateral Cauchy data at the boundary of a square. Because this square is a bounded domain, then the Lipschitz stability of the problem of [10] takes place [9, 7, 5], which is similar with the case of the above Inverse Problem 2.

Results of this paper provide a certain computational confirmation of the high degree of refocusing of time reversed wave fields in the presence of "*reflecting boundaries as waveguides or reverberating cavities*" (p. R2 in [3]), while Lipschitz stability estimates of [6, 9, 7, 5] might be viewed as ones providing a theoretical foundation of this experimental observation. On the other hand, Figure 9 displays solution of the φ-problem for $\varphi_*(x, y) = \delta(x - 0.9)\delta(y - 0.9)$ (i.e., for the same φ_* as above) and for the case when the Cauchy data are given only at the y-axis, i. e. at the line Γ_1 (see Figure 1). We have taken $\varepsilon = 0.3$ and 0.5, which is 30% and 50% the random noise in the data. We got $\|\boldsymbol{\varphi} - \boldsymbol{\varphi}_*\| = 0.36$ and 1.02, or 90% and 250% of relative error. It is clear that this result is much worse than one of Figure 8, although the noise level is less than in the previous case. Although an analog of the stability estimate of [6] (i.e., in the "continuous case") is not yet proven for the geometry corresponding to Figure 9, but numerical tests of Figure 9 indicate that such an estimate is likely much weaker than the Lipschitz estimate, because of different geometries

Acknowledgments

The work of M. V. Klibanov was supported by the grant W911NF-05-1-0378 from The US Army Research Office. The work of S. I. Kabanikhin and D. V. Nechaev was supported by grants 05-01-00559 and UR.04.01.026 from The Russian Foundation for Basic Research.

References

1. Bardos, C., Fink, M., 2002, Mathematical foundation of the time reversal mirror. Asymptotic Analysis, 29, 157-182

2. Borcea, L., Papanicolaou, G., Tsogka, C., Berriman, J., 2002, Imaging and time reversal in random media. *Inverse Problems*, **18**, 1247–1279.

3. Fink, M., Prada, C., 2001, Acoustic time-reversal mirrors. *Inverse Problems*, **17**, R1–R38.

4. Kabanikhin, S. I., Bektemesov, M. A., Nechaev, D. V., 2005, Numerical solution of the 2D thermoacoustic problem. *J. Inv. Ill-Posed Problems*, **13**, No. 3.

5. Kazemi, M., Klibanov, M. V., 1993, Stability estimates for ill-posed Cauchy problems involving hyperbolic equations and inequalities. *Applicable Analysis*, **50**, 93–102.

6. Klibanov, M. V., 2005, Lipschitz stability for hyperbolic inequalities in octants with the lateral Cauchy data and refocising in time reversal. *J. Inv. Ill-Posed Problems*, **13**, No. 4.

7. Klibanov, M. V., Malinsky J., 1991, Newton-Kantorovich method for 3-dimensional potential inverse scattering problem and stability of the hyperbolic Cauchy problem with time dependent data. *Inverse Problems*, **7**, 577–595.

8. Klibanov, M. V., Timonov, A., 2003, On the mathematical treatment of time reversal. *Inverse Problems*, **19**, 1280–1299.

9. Klibanov, M. V., Timonov, A. 2004, *Carleman Estimates for Coefficient Inverse Problems and Numerical Applications.* (Utrecht: VSP).

10. Klibanov, M. V., Rakesh, 1992, Numerical solution of a timelike Cauchy problem for the wave equation. *Math. Methods in Appl. Sci.*, **15**, 559–570.

11. Lattes, R., Lions, J.-L., 1969, *The Method of Quasi-Reversibility. Applications to Partial Differential Equations.* (New York: Elsevier).

12. Lavrentiev, M. M., Romanov, V. G., Shishatskii, S. P., 1986, *Ill-Posed Problems of Mathematical Physics and Analysis.* (Providence: AMS).

13. Tikhonov, A. N., Arsenin, V. Ya., 1977, *Solutions of Ill-Posed Problems.* (Washington, D.C.: Winston&Sons).

14. Vasil'ev, F. P., 1980, *Numerical Methods Of Solutions Of Extremal Problems.* (Moscow: Nauka) (in Russian).